

The application of stereoscopic PIV to measure the flow of air into an enclosure containing a fire

Rodney A. Bryant

Received: 19 June 2008 / Revised: 6 March 2009 / Accepted: 30 March 2009 / Published online: 22 April 2009
© US Government 2009

Abstract Flow fields encountered in full-scale enclosure fires are highly three-dimensional and span a large spatial extent. Stereoscopic particle image velocimetry (SPIV) was applied to provide a large-scale planar interrogation of the flow of air available to a series of fires burning inside an enclosure. Time-averaged velocity fields across the doorway of the enclosure are presented. These flows are bi-directional and SPIV reveals that the time-averaged height of the region of flow reversal depends on location within the doorway. The volume flow rate of available air computed from the classical one-dimensional flow approach agrees well with the numerical integration using the velocity field provided by SPIV. Good agreement between the measured velocities for SPIV configurations optimized for seed particle displacements along the laser sheet axis and optimized for displacements perpendicular to the laser sheet demonstrate that large-scale SPIV measurements can be conducted with very good precision.

1 Introduction

The release of heat due to fire causes the surrounding gases to move as a result of expansion and buoyancy. Far from the fire, very low speed flows are induced. In the case of a full-scale enclosure fire with a single vertical opening, such as a doorway, a counter-current flow results. A mixture of hot air and products from the fire escapes the enclosure

through the top of the doorway, while fresh air from the surrounding ambient environment flows into the enclosure through the bottom portion of the opening, as seen in Fig. 1. A region with lower pressure relative to ambient exists inside the lower layer of the room and the ambient air spills in. This is driven by the decrease in gas density resulting from the higher temperature in the upper layer of the room, and it is aided by the entrainment of air into the buoyant fire plume. Accurate measurements to quantify the gas exchange in enclosure fires between the ambient and the room interior are difficult due to the need to measure small gas velocities over a large spatial extent, while contending with the extreme conditions of the fire.

The flow through vents is three-dimensional and therefore a full mapping of the velocity and density fields is required to achieve the best accuracy for computed parameters such as mass flow rate. Due to the spatial extent of full-scale fire experiments, a complete velocity and density mapping of vent flows was not a feasible option for early investigations. Early efforts by Kawagoe (1958) and McCaffrey and Rockett (1977) to measure the ventilation of room fires employed only a few well-placed probes for differential pressure and temperature measurements. These studies relied on Bernoulli's equation and the assumption of one-dimensional flow. Later treatments by Steckler et al. (1982) and Nakaya et al. (1986) were improved by conducting differential pressure and temperature measurements with vertical arrays of bi-directional probes and bare-bead thermocouples, respectively. The vertical arrays were translated across the vents in order to characterize the three-dimensional nature of the flows.

The application of stereoscopic particle image velocimetry (SPIV) is a new approach to quantify the ventilation in enclosure fires. Its application to large-scale gas flows is difficult due to the need to balance the requirements for

R. A. Bryant (✉)
National Institute of Standards and Technology,
Building and Fire Research Laboratory,
Gaithersburg, MD 20899, USA
e-mail: rodney.bryant@nist.gov

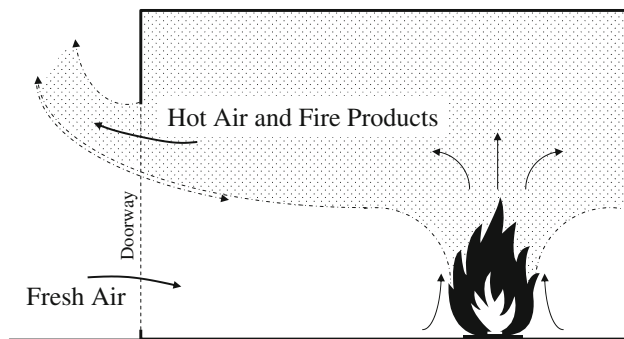


Fig. 1 Schematic illustration of the fire-induced flow in the doorway of an enclosure

accurate results with the availability of suitable tracer particles and the cost of lasers and CCD cameras. In spite of the difficulty, researchers have demonstrated that PIV can be successfully applied to study the intermediate and large-scale fire-induced flows. Probably the earliest work applying PIV to the study of small-scale fires is that of Zhou et al. (1996) who measured the velocity field in the surrounding air and near the base of 15 cm and 30 cm diameter liquid pool fires. Air entrainment rates were computed based on the mean velocity fields. The measured region was on the order of 10 cm by 14 cm and sub-micrometer Al_2O_3 particles provided adequate seeding. Tieszen et al. (2002) first demonstrated the application of PIV in large-scale fire experiments. They used cinematographic PIV to obtain simultaneous temporal and spatial resolution of a fire-induced flow. Measurements were conducted in the near field and on the centerline of a 1 m diameter methane flame with burning rates comparable to large pool fires. Due to the size of the measurement region, approximately 0.8 m by 1 m, tracer particles with a mean diameter of 60 μm were required to produce sufficient particle images for vector processing. The tracer particles were ceramic spheres, which survived the flame zones of the fire. Sun et al. (2005) conducted a comparison of a thermal PIV (TPIV) technique with traditional PIV by measuring the velocity field generated by a flame burning on a 8.8 cm diameter pool of alcohol. The TPIV technique uses “hot” pixels between successive frames of infrared images to simulate tracer particles. Velocity field data were collected over an area of 0.6 m by 0.4 m in the near-field region of the flame and surrounding air. Al_2O_3 particles were used to seed the flow due to their survival in the flame zone.

This paper presents SPIV measurements of the velocity field in the doorway of a standard size room containing a fire. This study is part of an ongoing effort at NIST to improve flow measurement techniques used in fire research. To the author’s knowledge this investigation is the first to apply SPIV to the study of fire-induced flow

through a doorway. This work is motivated by the need to apply measurement techniques independent of traditional physical probe measurements to the study of fire-induced flows. The work is also motivated by the need for experimental data obtained over the spatial scales of a full-scale enclosure fire (on the order of meters) combined with the spatial resolution required to provide validation for numerical simulation tools such as Large Eddy Simulation (LES) which is used extensively to predict fire growth and spread. This study focuses on the SPIV measurements of the flow of air into a room containing a fire. Velocity field measurements extend across the width of the doorway and are represented in terms of the three components, which allow for a more accurate computation of the volume flow of air into the room. A description of the experimental setup and methods follows. Conclusions drawn from the velocity data are also presented.

2 Experimental setup and methods

The developing stages of a fire inside a room were simulated using a standard enclosure and a natural gas burner. A constant flow of natural gas was delivered to the burner and ignited. The resulting fire generated a convective system that could be held at a thermal equilibrium for as long as the wall materials could survive. All experiments began at the minimum natural gas mass flow and the mass flow was increased to the specified set points in sequential order until the largest mass flow rate was achieved, Table 1. SPIV measurements were conducted at each set point after quasi-steady-state conditions inside the enclosure were achieved, that is after the effect of the initial transient had abated. The condition of quasi-steady-state inside the enclosure was determined by monitoring a thermocouple for relatively constant temperature. The thermocouple was located in the upper corner of the room $(x, y, z) = (0.81, 1.95, -0.62)$ m. Steady-state inside the enclosure was typically

Table 1 Statistics (mean \pm standard deviation) for natural gas mass flow, heat release, and internal thermocouple measurements over the set of repeat experiments

\dot{m}_{ng} , g/s	\dot{Q} , kW	T_r , K
0.72 ± 0.01	34.2 ± 0.3	371 ± 2
1.36 ± 0.02	64.8 ± 0.9	414 ± 2
2.01 ± 0.01	95.8 ± 0.3	454 ± 2
2.69 ± 0.01	128.6 ± 0.5	492 ± 2
3.35 ± 0.01	160.1 ± 0.7	529 ± 2
6.70 ± 0.02	320.2 ± 0.7	690 ± 3
10.70 ± 0.01	511.4 ± 0.2	865 ± 5

achieved within 20 min after reaching the mass flow set point.

Nine repeat experiments were conducted for each fuel flow rate except for the largest fuel flow rate. The total number of fires was 58; 9 repeats for all fires up to 320 kW and 4 repeats for the 511 kW fire (sustainability of the structure became an issue at 511 kW). The mean and standard deviation over the set of repeat measurements are listed in Table 1 for the natural gas mass flow rate, \dot{m}_{ng} , heat release of the fire, \dot{Q} , and thermocouple temperature inside the room, T_r . The results demonstrate the excellent repeatability that was achieved for generating the natural gas fires and the conditions inside the enclosure. The standard deviation of the thermocouple reading after 20 min is less than $\pm 1\%$ of the mean for all conditions. SPIV measurements were conducted for all 58 fires. The experiments were conducted in the Large Fire Laboratory at NIST. Estimated measurement uncertainties and the standard deviation of the repeat experiments are reported. All measurement uncertainties are for a 95% confidence interval.

2.1 Enclosure fires

The experiments were designed to be similar to those of Steckler et al. (1982) which have been the most detailed characterization of fire-induced flows in a doorway. Experiments were performed using a standard fire test room which conformed to the specifications for physical dimensions as stated in the International Organization for Standards (ISO) 9705 standard (1993). The enclosure is a full-scale room used to evaluate wall surface products for their contribution

to fire growth, Fig. 2. The interior dimensions of the room were $(3.60 \times 2.40 \times 2.40) \pm 0.04$ m (length \times width \times height). Drywall (gypsum board) lined the lower half of the vertical walls and the floor of the enclosure while calcium silicate panels lined the upper half of the vertical walls and the ceiling to withstand the high temperatures for longer periods. Both materials were applied in two layers, resulting in a wall thickness of 2.5 cm. A doorway was located on the center of one of the 2.4 m \times 2.4 m walls and served as the only vent for the enclosure. The dimensions of the doorway, $(0.79 \times 1.96) \pm 0.01$ m ($W \times H$), were similar to that of a standard interior doorway. The depth of the doorway, D , was 0.30 ± 0.01 m with the doorway protruding from the exterior wall. This configuration was necessary to accommodate a window mounted on one side of the doorway through which the laser sheet passed across the doorway for the SPIV measurements. In this configuration, the limits of integration for a direct computation of volume flow rate are defined by the intersection of the laser sheet and the solid boundaries of the door frame. A rectangular coordinate system was adopted and its origin $(0, 0, 0)$ was located at the floor of the doorway and at the geometric center of the horizontal plane defined by the width of doorway and the depth of the door jamb. The ISO 9705 room sat on a platform equipped with castors for positioning the room in the laboratory. The floor of the ISO 9705 room was 0.29 ± 0.01 m above the laboratory floor.

The experiments were run under an exhaust hood designed to remove the combustion products from fires up to 500 kW. An exhaust rate of 1.89 ± 0.19 m³/s was adequate to remove the products for a 511 kW fire and does not impart a significant influence on the ambient flow that entered the enclosure. During preliminary tests theater fog was seeded into the ambient air. By visual inspection of the fog, the exhaust rate was tuned to the lowest setting that would not cause the fog to rise faster than it could be drawn into the room while ensuring that all fire products were exhausted. This exhaust setting was utilized for all experiments. The rectangular hood had dimensions of $(3.35 \times 3.35) \pm 0.01$ m (length \times width) and was supported by four steel pillars that rested on the laboratory floor. Walls which extended to the floor were constructed on two sides of the exhaust hood while the ISO 9705 room was placed adjacent to one side of the exhaust hood. This arrangement closed off the area under the exhaust hood except for one side which remained open, therefore creating a vestibule for the ambient air to pass through before entering the doorway of the ISO 9705 room. Preliminary flow visualizations indicated that flow currents in the laboratory were significant to cause asymmetry in the flow through the doorway. For this reason the vestibule was constructed to channel the flow toward the door and reduce the cross currents. Seed particles were dispersed into the ambient air inside the vestibule.

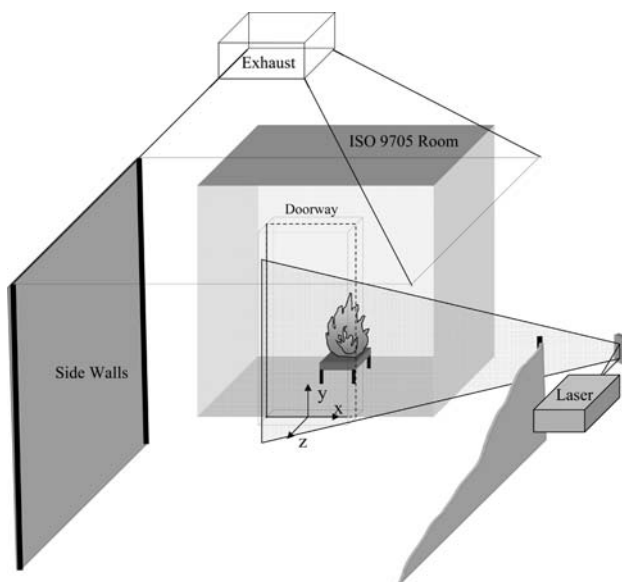


Fig. 2 Schematic illustration of the enclosure fire experiment and SPIV setup

Fires were generated using a gas burner placed in the center of the floor of the ISO room. The burner was a square steel pan, $(30.5 \times 30.5 \times 7.0) \pm 0.2$ cm, filled with a porous ceramic material to generate a uniform flow at the burner exit. The top of the burner was elevated 30.0 ± 0.2 cm above the floor of the enclosure. Natural gas entered the bottom of the burner and dispersed through the porous material before being ignited to produce a fire that spanned across the top surface of the burner. The volume flow rate of natural gas was measured by a rotary displacement meter upstream of the burner. Assuming complete combustion of the natural gas, the real-time heat output of the burner was computed using the measured volume flow rate corrected for local conditions and the heat of combustion of natural gas. The resulting mass flow of natural gas ranged from 0.72 to 10.70 g/s, generating fires ranging from 34 to 511 kW, respectively. The estimated relative uncertainty of both the mass flow of natural gas and energy release from the fires is ± 0.02 , Bryant and Mulholland (2008). Combustion efficiency measurements above 98% have been reported for similar burners used in this laboratory, Bundy et al. (2007). Their measurements were conducted for fires ranging from 75 to 425 kW.

2.2 SPIV system

Stereoscopic PIV was used to measure the velocity of air through the doorway and hence available to the fire inside the enclosure. Two laser sheet configurations were used. In the first configuration the laser sheet propagated across the vertical plane of the doorway. It spanned across the entire width (0.79 m) of the doorway and spanned the lower 92% (1.80 m) of the doorway height. Because the flow of ambient air into the room occurs through the lower portion of the doorway, each fluid element containing ambient air that entered the enclosure was required to cross the plane defined by the laser sheet, Fig. 2. In this configuration (A), the bulk flow of fluid through the doorway was perpendicular to the laser sheet, Fig. 3. Therefore, the particle displacements perpendicular to the laser sheet were the greatest. Conventional PIV is only capable of recording two-dimensional projections of the three-dimensional displacements in the plane of the laser sheet. Information for the particle displacements normal to the plane is lost. By adding a second camera to record an additional PIV image of the same field of view but from a different viewing angle, hence the name stereoscopic PIV, the information for the particle displacements normal to the plane can be recovered. Images of a calibration target can be used to create a model of how each camera images the flow field. In turn this model is used to reconstruct the three-dimensional displacement vectors from the two-dimensional projections. The SPIV technique and its advantages have

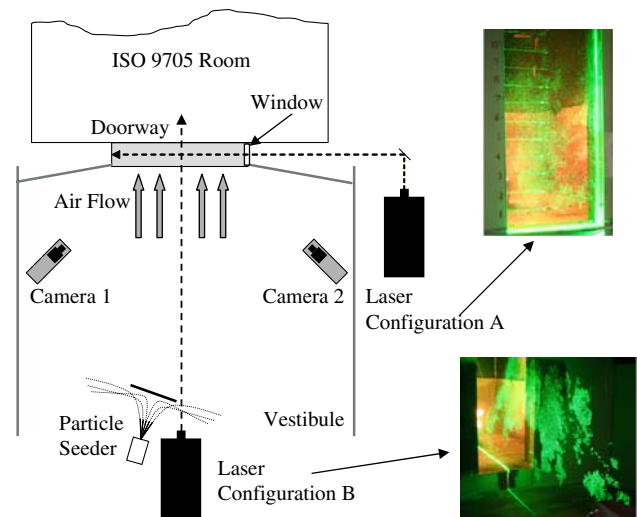


Fig. 3 Schematic illustration of the SPIV system—configurations A and B

been described in depth by Raffel et al. (1998) and Prasad and Adrian (1993). To provide a confirmation measurement for the velocity field, a second configuration (B) of the laser sheet was used. In this configuration the laser sheet propagated along the centerline of the doorway and perpendicular to the doorway plane. Particle displacements due to the bulk flow direction were in the plane of the laser sheet, Fig. 3. The two configurations of SPIV measurements allow for a comparison of the same displacement vector component but each reconstructed from a different set of two-dimensional projections.

The SPIV system illustrated in Fig. 3, a commercial system from LaVision, Inc.,¹ used twin Nd:YAG lasers as the illumination source. Each laser issued a pulse at a rate of 10 Hz and frequency doubled to a wavelength of 532 nm (200 mJ/pulse nominal). A sheet forming optics assembly with a -10 mm focal length cylindrical lens was attached to the laser head to spread the beam into a sheet. The laser sheet passed through a window on one side of the doorway and was absorbed by rhodamine paint on the opposing wall. The rhodamine paint was excited by the 532 nm laser light and emitted fluorescence in a wavelength band shifted toward the infrared. The thickness of the laser sheet was estimated to be 1.2 ± 0.3 cm as determined by measuring the thickness of the visible fluorescence on the opposing wall. This sheet thickness was required when the bulk flow was perpendicular to the

¹ Certain commercial entities, equipment, or materials may be identified in this document in order to describe an experimental procedure or concept adequately. Such identification is neither intended to imply recommendation or endorsement by the National Institute of Standards and Technology, nor is it intended to imply that the entities, materials, or equipment are necessarily the best available for the purpose.

laser sheet to prevent particles from leaving the measurement region before completion of the measurement. With the sheet aligned parallel to the bulk flow, configuration B, particle loss would be less for measurements on the centerline of an ideally symmetric flow. In the case of an ideally symmetric flow, the sheet thickness could have been reduced to increase laser intensity and therefore increase the particle scattering signal. Because the scattering signal from the particles was sufficient, the same sheet thickness was applied in configuration B as a safety precaution against particle loss. Precise positioning of the laser sheet at the doorway was performed by a 45° mirror attached to a translation stage.

Digital images were acquired with two identical 12 bit CCD cameras at a rate of 1.0 fps (PIV capture rate, maximum camera frame rate = 16 fps). The CCD sensor pixel format was 2,048 × 2048 pixels with single pixel dimensions of 7.4 μm on a side. Wide angle lenses (Nikon Nikkor 20 mm focal length) were used to capture a field of view of 1.7 m × 2.3 m (width × height). The final region of interest, 0.8 m × 1.5 m (configuration B: 1.8 m × 1.9 m), was defined by the span of the laser sheet across the doorway and the presence of seed particles in the upper reaches of the doorway. The cameras were positioned symmetrically about the doorway with an angle of approximately 80° between the two cameras (configurations A and B). In this configuration the cameras were not perpendicular to the laser sheet plane and the image focus was reduced toward the edges of the field of view. The lenses were mounted in Scheimpflug adapters which allow for a wider range of focus by tilting the lenses until the Scheimpflug criteria is met; the image plane, lens plane and object plane intersect in a line. This was achieved empirically by tilting the lenses while viewing the calibration target until it was entirely in focus. Satisfying the Scheimpflug criteria was necessary to record adequate particle images in the entire field of view. Each camera assembly was placed in a protective housing that was purged with air in order to reduce their exposure to the seed particles and the heat of the fire. Laser line filters (532 nm) were attached to the lenses to reduce the interference from the visible radiation of the fire and the ambient lighting.

A pneumatic paint sprayer served as the particle seeder shown in Fig. 3. The particles were ejected as a fine spray into the large quiescent flow inside the vestibule. A plate was placed in front of the paint sprayer and perpendicular to the axis of the jet in order to redirect the momentum of the particle spray to be closer to normal to the direction of the bulk flow into the doorway. The seeded air was drawn into the enclosure through the doorway and once inside the enclosure the air was directly entrained into the fire plume and mixed into the flow of the upper layer of the room. A good portion of the flow out of the doorway was seeded

with tracer particles due to the flow mixing that occurred inside the room. Therefore, a single paint sprayer was sufficient to seed the region of interest for the present investigation. Cyclic bursts of the particle spray were produced using an electronic trigger pulse from the PIV timing unit. The pulse triggered solenoid valves to release high-pressure air that engaged a pneumatic actuator attached to the lever of the paint sprayer and the high-pressure air carrying the particle spray. Photographs which capture the scattered laser light from the seed particles are shown in Fig. 3 for both laser configurations.

The seed particles were dry expanded microspheres (Expancel 092 DET 120 d30). The microspheres are hollow plastic shells made of a copolymer and enclosed in each plastic shell is a gas such as isopentane. The weight mean particle diameter ranges from 100 to 140 μm and the particle density is 30 kg/m³. The estimated terminal velocity of a 140 μm particle at room temperature is 0.02 m/s. It will decrease for smaller particles and higher gas viscosity and is estimated to be 0.01 m/s for a 100 μm particle in air at 460 K. The gas composition in the upper portion of the doorway was assumed to be mostly air. The particles rupture and begin to decompose at temperatures above 460 K (190°C), therefore seeding was not possible in the upper regions of the flow. Likewise the particle response time will be greatest for large particles in room temperature air and less for small particles in air at elevated temperatures. Estimates of particle response time (time required to reach 63% of flow velocity) range from 0.6 to 1.8 ms. The time between PIV frames ranged from 2 to 10 ms, therefore the particles had enough time to catch up to the flow before the measurement was completed.

A commercial PIV system is capable of measuring the displacement of a particle with an uncertainty of 0.01 pixels. Experiments were conducted to compare measured displacements to known displacements for the same optical configuration employed in the present study. Measured displacements agreed with known displacements to within 0.01 pixels or less. For the optical magnification and laser pulse separation times employed in the present study, the uncertainty of the SPIV velocity measurements is estimated to be ±0.006 m/s for the horizontal components of velocity, v_x and v_z . The vertical component of velocity, v_y , has additional uncertainty due to the terminal velocity of the particles. Its uncertainty is estimated to be ±0.026 m/s.

At each fire condition 200 SPIV image sets were acquired. The vector fields were computed using the manufacturer provided software, DaVis 7.1. A background image was subtracted from each image to increase the signal-to-noise ratio. The background image was created by averaging the images from the data ensemble. An adaptive stereo cross-correlation was applied to each

image—three evaluation passes with decreasing interrogation windows and 50% overlap. Spurious vectors were removed on each pass using a 3×3 median filter. The final interrogation window size was 32 pixels \times 32 pixels which corresponded to a spatial resolution of 4 cm \times 4 cm and a vector spacing of 2 cm \times 2 cm. A custom stereo calibration plate with marks on two levels was used to obtain the geometrical information necessary to convert image dimensions to pixel units. The dimensions of the calibration plate were 0.75 m \times 1.15 m (width \times height) and therefore did not span the entire measurement region. The self-calibration feature of DaVis 7.1, Wieneke (2005), was applied to ensure accurate vectors outside of the initial calibration space and to correct for misalignment between the calibration plate and the laser sheet. Mean vector fields were computed from the 200 image data ensemble. Homogeneous seeding of the entire measurement region was difficult to achieve for a single instantaneous PIV image acquisition, therefore some instantaneous vector fields contained regions without valid vectors. Computation of a mean vector required a minimum of ten valid vectors at that location.

3 Results and discussion

The velocity field across the width of the doorway (configuration A) for selected fire conditions is displayed in Fig. 4. Mean velocity vectors are plotted. The velocity components parallel to the laser sheet, v_x and v_y , are displayed as vectors and the component normal to the laser sheet, v_z , is displayed as a color map. The flow of ambient air into the room is represented by the blue shaded region, negative v_z , while the flow of hot gases out of the room is represented by the red shaded region, positive v_z . The normal velocity component passes through zero at the interface of the two flows and is represented as a narrow green band. The seed particles did not survive in the hottest regions of the flow and therefore SPIV measurements could not be acquired in the upper regions of the doorway and only the lower part of the flow out of the room is displayed in the figures. Velocity vectors could not be acquired very close to the solid boundaries. Between the region of valid vectors and the solid boundary any spurious vectors were removed and the no-slip condition was applied at the boundary. To fill these regions with reasonable vectors a two-dimensional cubic interpolation between the region of valid vectors and the no-slip boundary was applied. The average interpolation distance at both the vertical and horizontal solid boundaries was 2 cm, with a maximum distance of 4 cm. The average interpolation distance was the same as the measurement spacing. At the bottom left

and right corners the average interpolation distance was 2 and 8 cm, respectively, in either direction.

In Fig. 4, the size of the fire increases, from left to right, while the size of the area of flow into the room (blue) decreases. This is due to the volumetric expansion of hot gases occurring at the flame, which forces gas into the upper layer of the room and out of the room through the opening, increasing the area available for flow out of the room. In both regions, outflow and inflow, the velocity magnitude increases with increasing energy release from the fire as demonstrated by the darkening of the shaded color regions and the increases in vector length. The interface of the two flows, the narrow green band across the width of the doorway, is more of a curved surface rather than a flat plane, revealing that the height of the flow interface, h , is a function of the position, x , across the width of the doorway. The curvature of the interface decreases with increasing fire size.

The flow of air into the room is inherently laminar. It originates from the mostly quiescent ambient air in the laboratory. The flow out of the room has origins from the buoyant plume due to the fire and is turbulent in nature. Therefore, it is expected that the interface of the two flows will provide some evidence of the turbulent behavior of a doorway flow. Qualitative evidence is presented in the instantaneous vector fields in Fig. 5. The vector fields come from sequential PIV images with good seeding over the entire measurement region. The vector fields displayed in Fig. 5 were post-processed using three passes of a 3×3 smoothing filter and a linear interpolation to fill empty spaces. This level of post-processing improves the appearance of the vector fields while preserving the qualitative information from the raw vector fields. The flow interface has significant structure to its underlying curved shape defined by the mean vector fields of Fig. 4. This structure results from intermittent large-scale structures of the flow issuing from inside the room as well as from vortical structures produced at the interface of the two counter-current flows. The vector fields in Fig. 5 come from the 160 kW fire experiments and were selected to demonstrate the general characteristics of the instantaneous flow structure.

Horizontal profiles of the velocity components are plotted in Fig. 6 for selected elevations. Profiles measured for the conditions of the 160 kW fire are displayed and are representative of the general characteristics of the profiles. The profiles demonstrate the significant variation in each component of velocity with respect to position in the doorway. The profiles also demonstrate that the flow is nearly symmetric about the vertical axis. For the v_x profiles the symmetric features for the flow into the room are opposite to those features for the flow out of the room. The measurement plane is closer to the room exterior therefore

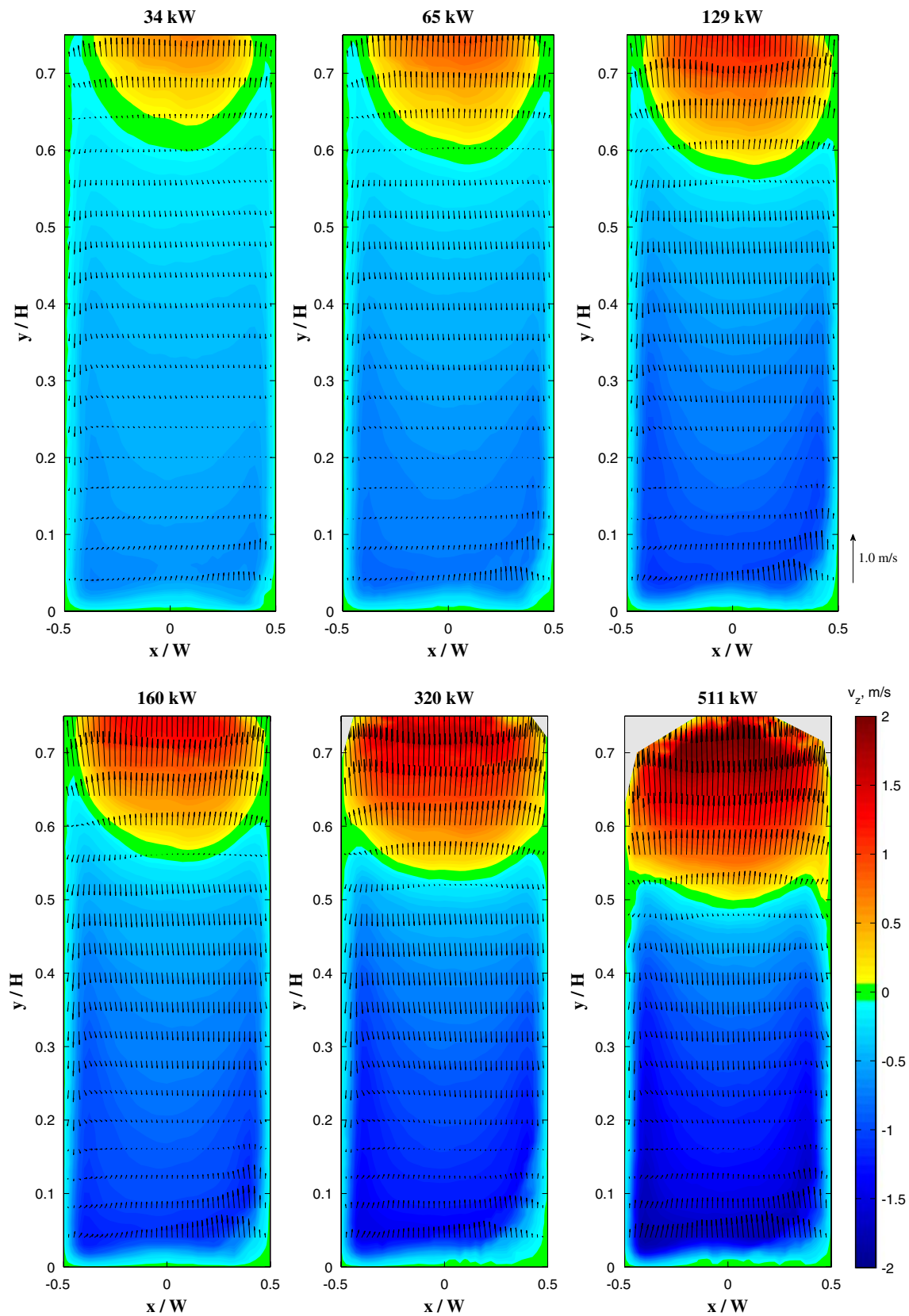


Fig. 4 Mean velocity field across the doorway plane (xy plane, at $z = 0.05$ cm), configuration A. Fire size (i.e. natural gas mass flow rate) increases from left to right. SPIV results were obtained for the lower 75% of the doorway height

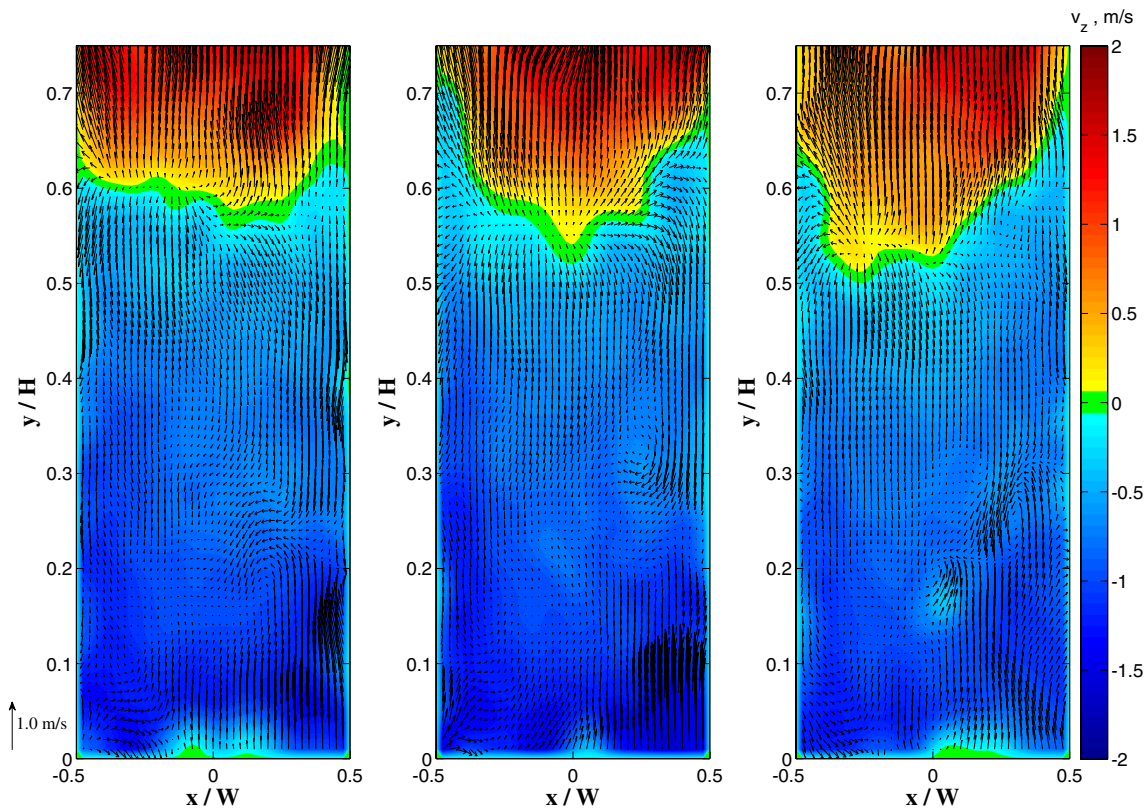
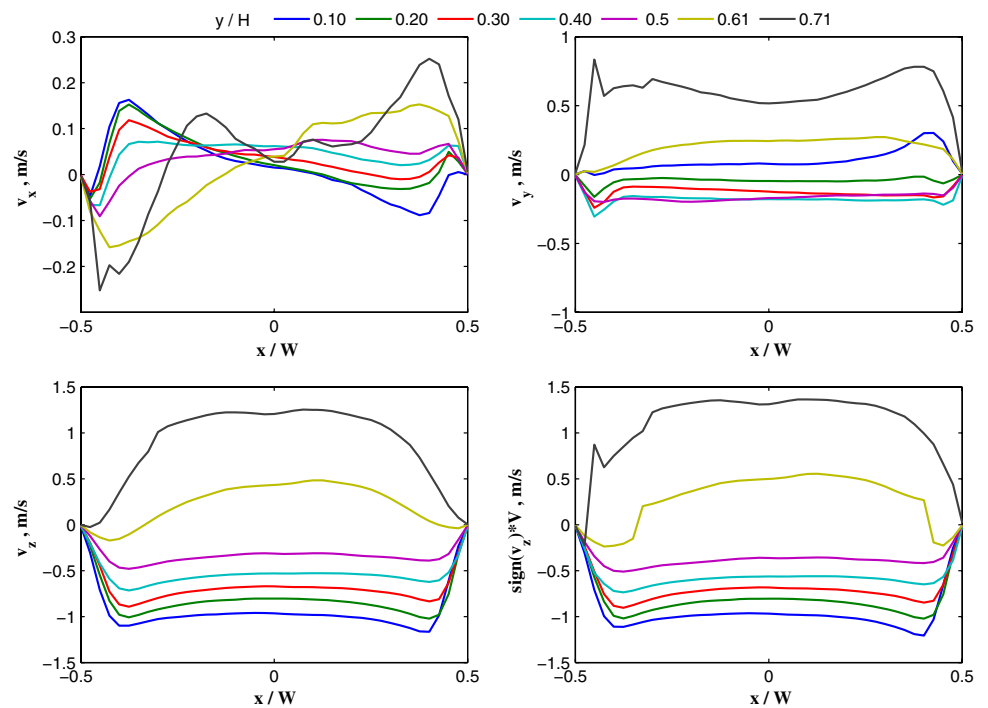


Fig. 5 Instantaneous vector fields across the doorway plane (xy plane, at $z = 0.05$ cm), configuration A, 160 kW fire. Starting at the *left*, the images are sequential and separated in time by 1.0 s

Fig. 6 Horizontal profiles of velocity components and velocity magnitude for the 160 kW fire ($\dot{m}_{ng} = 3.35$ g/s), $\text{sign}(v_z) = 1$ for $v_z > 0$, $\text{sign}(v_z) = -1$ for $v_z < 0$



capturing the flow convergence from the ambient toward the doorway and the flow divergence from inside the room to the ambient. The v_y component of velocity is positive for

the flow out of the room due to the buoyancy of the plume issuing from the doorway. Negative v_y is observed for the flow into the room except near the bottom of the doorway.

The room stands above the laboratory floor and the flow must step up into the room. Much of the upward momentum of the flow remains at this measurement location.

Horizontal profiles of v_z are consistent with the color contours of Fig. 4. For the flow into the room, negative v_z , the magnitude of v_z is the greatest near the solid boundaries of the doorway and goes through a minimum near the centerline. These profiles are characteristic of the flow across an orifice that originated as an ideal flow at rest. Similar velocity profiles were reported by Steckler et al. who traversed a vertical array of differential pressure probes across the doorway of a comparable sized room. The profiles for velocity magnitude are almost identical to v_z profiles for the flow into the room, where v_z dominates the contribution to the velocity magnitude. However, the profiles are flatter for the flow out of the room due to a significant contribution from the v_y component.

The general characteristics of a fire-induced flow across an opening can be described by treating the flow as incompressible, inviscid, and driven by buoyancy. The buoyant fire plume acts as a source to push gas into the upper layer and out of the enclosure while simultaneously acting as a sink to draw gas into the doorway and into the lower layer of the enclosure. Much of the literature (Steckler et al. (1984), Steckler et al. (1982), Rockett (1976), Prahl and Emmons (1975)) has demonstrated that the details of the plume can be ignored when treating the flow at the doorway. Instead, a simple hydrostatic treatment based on the temperature difference between the interior of the room and the ambient is sufficient to describe the flow at the doorway. By treating the conditions created by the fire, the fire-induced flow through the doorway is analogous to and somewhat an extreme case of the natural convection flow that continuously occurs in buildings. Dalziel and Lane-Serff (1991) and Linden (1999) describe such natural convection flows by dividing the interior of the room into two layers, a hot upper layer and a cold lower layer. The upper layer is buoyant and wants to escape the room across the top of the opening while the lower layer is continuously supplied with cool air from the ambient environment flowing across the bottom of the opening. Within the two layers gas temperature is vertically distributed with the temperature increasing as the distance from the floor increases. Gases will move from a hot room to a cooler room, so for a general description of the flow across the doorway it is practical to assume that the temperature and density field inside the room is independent of vertical position. The hydrostatic pressure difference across the doorway, ΔP , is induced by the density difference, $\Delta\rho$, between the room interior and the ambient and is described as $\Delta\rho gy'$ at each vertical position. The interface of the flow into the room and out of the room serves as a reference location and y' is the vertical distance

in either direction away from the interface, while g is the acceleration due to gravity. Assuming an incompressible and inviscid flow, Bernoulli's equation can be used to describe the local velocity, $\sqrt{2gy'\Delta\rho/\bar{\rho}}$, with $\bar{\rho} = (\rho_r + \rho_a)/2$ being the average density between the room interior and the ambient. For an ideal gas the density ratio, $\Delta\rho/\bar{\rho}$, is equal to the negative temperature ratio, $-\Delta T/\bar{T}$, with $\bar{T} = (T_r + T_a)/2$. Therefore, the local velocity magnitude at the opening can be generalized by the following equation.

$$V = \sqrt{2gy'\Delta T/\bar{T}} \quad (1)$$

This relation describes the velocity magnitude of both inflow and outflow. The velocity is zero at the flow interface, $y' = 0$, and increases with increasing distance away from the interface. The velocity magnitude also increases with increasing fire size due to the increasing difference in temperature between the room and the ambient environment.

Vertical profiles of the velocity magnitude, V , computed from the SPIV measurements are presented in Fig. 7 for the centerline of the doorway. The profiles are multiplied by the sign of v_z at each vertical location in order to retain directional information of the flow. Below the flow interface, the profiles obey the generalizations of Eq. 1, with flow speed increasing with increasing vertical distance from the flow interface and with increasing fire size, therefore increasing ΔT . At the maximum fire size, nominally 511 kW, the flow speed on centerline was as high as 1.70 m/s into the room. At the minimum fire size, nominally 34 kW, the highest flow speed on centerline into the room was 0.60 m/s. For the flow into the room the highest

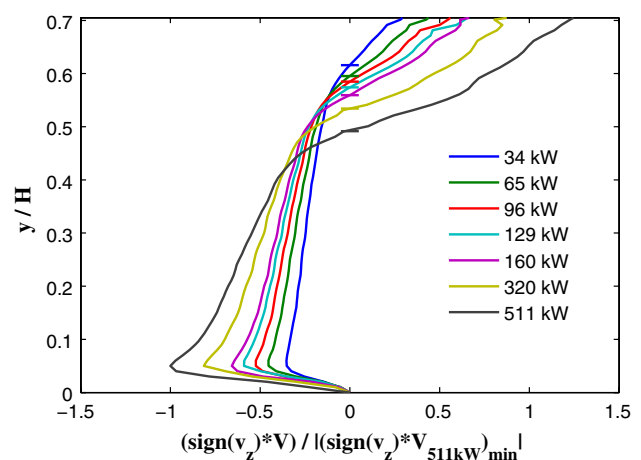


Fig. 7 Centerline vertical profiles ($x = 0.0$ m, $z = 0.05$ m) of the velocity magnitude, V , normalized with respect to the fastest flow into the room, 1.70 m/s, at the maximum heat release, 511 kW. The short horizontal lines are the mean location of the flow interface. [$\text{sign}(v_z) = 1$ for $v_z > 0$, $\text{sign}(v_z) = -1$ for $v_z < 0$]

flow speed on the centerline occurs consistently near the floor in a region surrounding $y = 0.05H$.

Flow interfaces with uniform height across the doorway were reported by Steckler et al. compared to the parabolic shaped interfaces observed with the SPIV measurements. The interface of the inflow and outflow has been described previously as a flat plane, the neutral plane, at which the velocity magnitude, V , is zero. Previous methods for observing the neutral plane used video of smoke layers or vertically spaced bi-directional pressure probes to detect the change in sign of the differential pressure. The SPIV measurements show this region to be more of a curved surface, especially for low-energy fires. Accurately locating the interface region is critical to define the area of integration for computations of total flow into and out of the enclosure. The mean location of the interface along the vertical axis of the doorway, $x = 0.0$, is presented in Fig. 8. The standard deviation of the repeat experiments was less than 2% of the mean height for all conditions except the lowest energy fire, where it ranged from 2 to 3%.

In the present experiments the door jamb has a depth of 30 cm. SPIV measurements of the velocity field on the centerline of the doorway, configuration B, reveal that the interface height decreases with position inside the door jamb and inside the room. Figure 8 demonstrates that the height of the interface region decreases by 20% over the 30 cm ($-0.15 \text{ m} \leq z \leq 0.15 \text{ m}$) that define the horizontal depth of the door jamb. At $z = 0.0 \text{ m}$ the interface height ranges from $0.60H$ to $0.48H$, for the nominally 34–511 kW fires respectively. This result agrees well with Steckler et al. who reported a range of $0.58H$ – $0.54H$ for nominally 32–158 kW fires in a room of similar dimensions. Figure 8

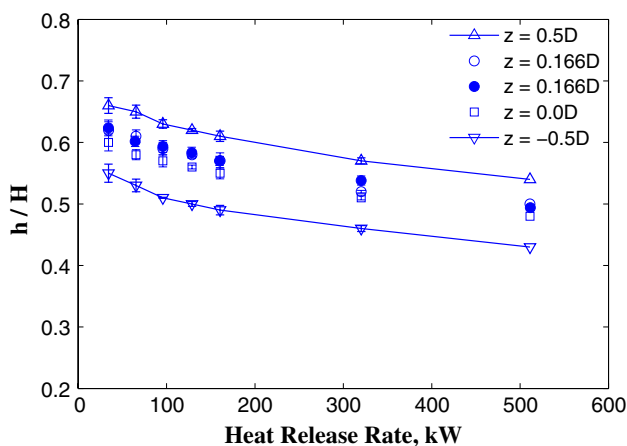


Fig. 8 Mean location of flow interface at the doorway horizontal axis, $x = 0.0 \text{ m}$. Closed symbols represent configuration A results, open symbols represent configuration B results. The standard deviation over the repeat experiments is represented by the error bars

demonstrates that the measurement position within the depth of the doorway is significant in determining the interface height.

The SPIV measurements from configuration A allow for a computation of the volume flow rate of air into the room never before achievable with conventional physical probe measurements. This configuration allows for the precise determination of the cross-sectional area of the flow. It provides an increase in spatial sampling and resolution which reduces the need to assume one-dimensional flow. It also allows for the velocity component normal to the plane to be measured, therefore not relying on the assumption of a single velocity component flow. The most accurate computation of volume flow rate across an opening is an integration of the normal component of velocity over a cross-sectional area with limits of integration defined by the solid boundaries, $\int_0^H \int_{-W/2}^{W/2} v_{\perp} dx dy$. In the case of the fire-induced bi-directional flow through the doorway, the flow is considered in two parts; flow into the room and flow out of the room. Since both flows occur in the same opening, the horizontal limits of integration for both flows are defined by the width of the doorway. The height of the flow interface, $h(x)$, defines the upper vertical integration limit for the flow into the room and the lower vertical integration limit for the flow out of the room. Consider the blue regions of Fig. 4 which represent the average flow into the room, i.e. negative v_z . Integrating v_z across this area results in the computation of the volume flow rate of air into the room. Volume flow rates of air flowing into the room computed from the SPIV measurements are shown in Fig. 9. The flow of air into the room increased with increasing fire strength. The rate of increase slows for the larger fires due to the size of the opening limiting the flow

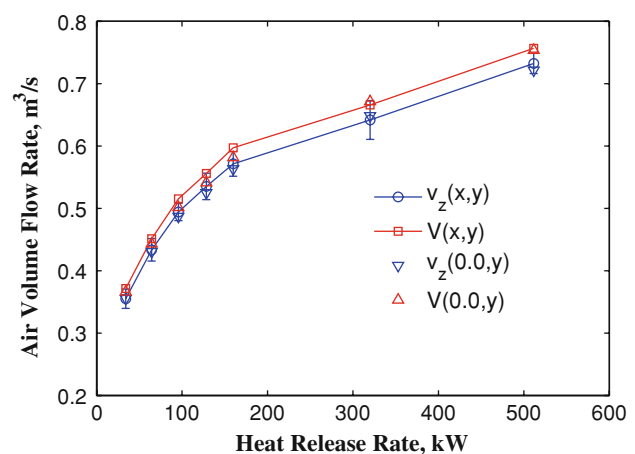


Fig. 9 Volume flow rate of air into the room computed from SPIV measurements of v_z and velocity magnitude, V . Velocity data come from the doorway cross section at $z = 0.05 \text{ m}$ (configuration A). Volume flow rate computed using the vertical profile on centerline, $v_z(0.0, y)$ and $V(0.0, y)$, is represented by the triangles

of air into the room. The standard deviations of the repeat experiments range from 2 to 4% of the mean value. This is a very good repeatability considering that homogeneous seeding of the measurement region was difficult to achieve for each instantaneous PIV acquisition. This demonstrates that 200 samples of the instantaneous velocity field were sufficient to compute accurate average velocity fields.

The most direct computation of volume flow rate is performed using v_z , the normal velocity component to the opening. Bi-directional pressure probes are commonly used in fire experiments to measure flow velocity, McCaffrey and Heskestad (1976). These probes were designed to limit clogging by soot and debris and sensitivity to the angular direction of the flow. As a result the probes have large pressure taps and flow stagnation regions. Their response is more characteristic of the flow speed than the velocity along the axis of the probes. Volume flow rate computed using the flow speed, V , from the SPIV measurements is also shown in Fig. 9. The computation is analogous to traversing a vertical array of physical probes that respond to flow speed across the width of the doorway. Assuming that the probe measurements agreed exactly with the SPIV measurements, this method would overestimate the most direct computation by only about 4%. The speed of the flow into the room is dominated by v_z , but there are regions of the flow where v_x and v_y contribute significantly to the flow speed as demonstrated in Figs. 4 and 6.

In large fire experiments it is common practice to assume that the flow through the doorway is constant in the horizontal direction and therefore only measurements from a vertical array at the doorway center are sufficient to describe the flow. This assumption greatly reduces the number of required measurements when using physical probes. The volume flow rate computed based on this assumption is the product of the doorway width and an integration of the vertical velocity profile on centerline with the integration limits defined by the doorway sill, $y = 0.0$ m, and the flow interface height, $h(x = 0.0)$. The discrepancy between volume flow rate computed using centerline profiles and that computed using the entire flow field is less than 2 and 3% when the integrand is v_z and V , respectively. This result suggests that the centerline velocity at each elevation is representative of the average velocity along the width of the doorway despite the fact that Figs. 4 and 6 demonstrate that there is significant change in the flow across the width of the doorway. The result also suggests that the curvature of the flow interface has only a small impact on the volume flow rate computation.

The SPIV measurement results for configuration B are displayed in Fig. 10. The vector field represents the velocity components in the plane of the laser sheet, v_x and v_y , while the color map shows flow speed. The velocity component

perpendicular to the yz plane, v_x , is small on centerline, ranging from -0.25 to 0.2 m/s and is therefore not shown. Similar to Fig. 4 the increase in the size of the region of the flow out of the room (red) with increasing fire size demonstrates how the expansion of the hot gases within the room affects the structure of the flow through the doorway. This configuration provides another perspective from which the change in the velocity field with increasing energy release rate from the fire can be observed. In the ambient and far from the doorway the flow speed is slow and mostly horizontal. The flow of air accelerates through the doorway and is directed toward the floor as it progresses into the room. These figures demonstrate that there is a significant vertical component to the velocity vector for both flow out of the room and flow into the room. The hot gases escaping out of the room are highly buoyant, and the vertical component of velocity, v_y , is significant. For the limited region of measurements in the upper portion of the doorway, v_y can be as much as 50–90% of v_z . Measurements in the remaining upper region of the doorway are needed to determine if this observation will hold true for the entire field of flow out of the room. The interface of the two flows is displayed as a narrow green band between the red and blue regions as shown in Fig. 4. As discussed previously, the interface location varies significantly with position along the depth of the doorway and Fig. 10 demonstrates that this is true inside the room also, $z < -0.5D$.

Instantaneous vector fields for configuration B are presented in Fig. 11 to demonstrate the general characteristics of the instantaneous flow structure along the direction of the bulk flow. Like Fig. 5, the vector fields were computed from sequential PIV images with good seeding over the entire measurement region and the same post-processing steps were applied. Again the flow interface shown in Fig. 11 has significant structure to its underlying linear shape defined by the mean vector fields of Fig. 10. Comparing the first and last vector fields in the sequence of Fig. 11, the horizontal extent of the flow interface across the depth of the doorway and therefore the extent to which it protrudes from the doorway is intermittent. Flow circulation is also observed at the flow interface for this configuration of the SPIV measurements. The circulation confirms the presence of vortical structures at the interface of the counter-current flows.

Measurements in configuration B were conducted to provide a confirmation measurement of v_z and to provide information on the evolution of the velocity field from the room exterior, through the doorway, and into the room. In this configuration, the laser sheet orientation was in the yz plane and it propagated from the room exterior into the interior along the centerline of the doorway. The primary direction of the flow through the doorway was parallel to the laser sheet and the resulting particle displacements

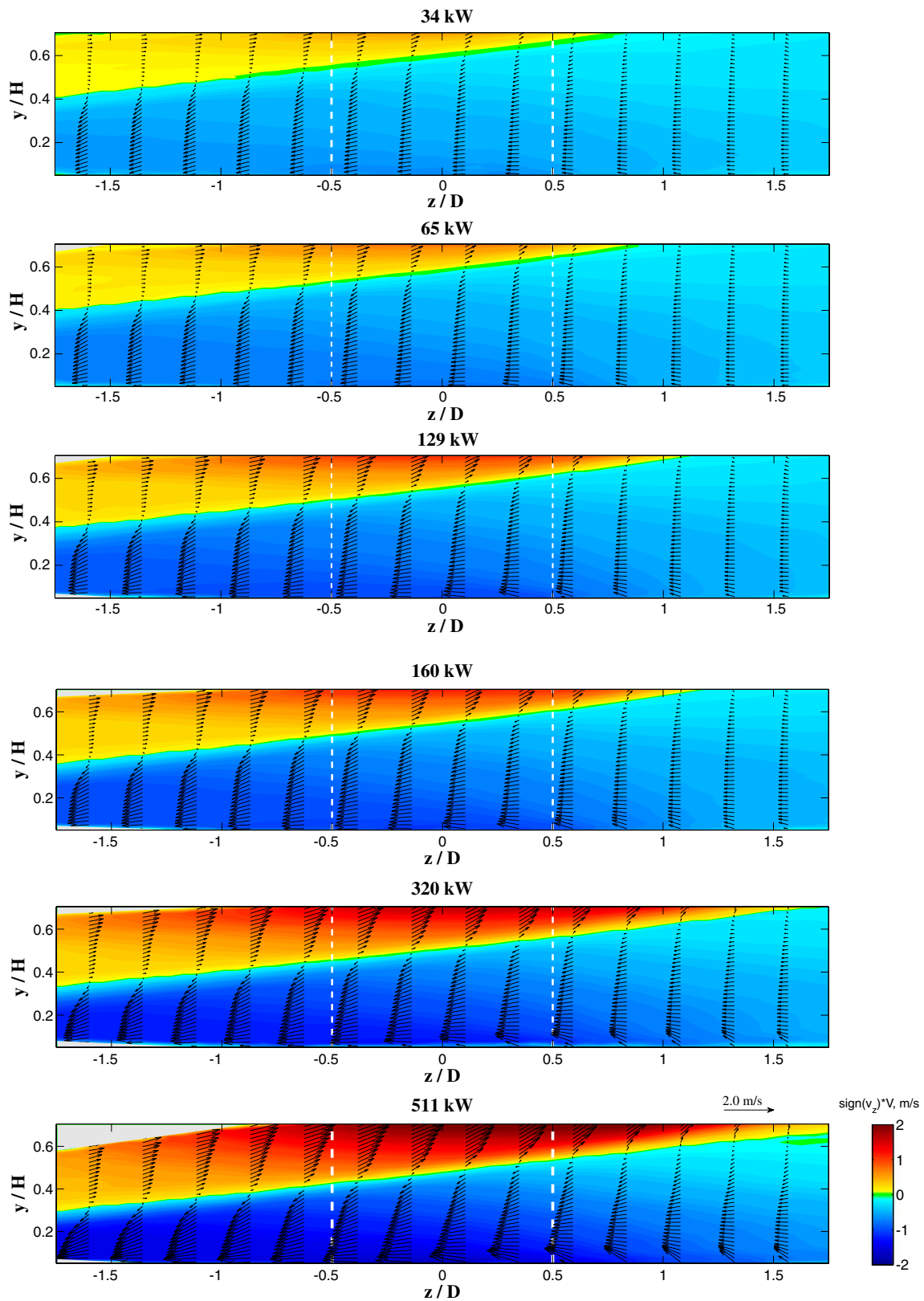


Fig. 10 Mean velocity field along the centerline of the doorway (yz plane, at $x = 0.0$ m), configuration B. Fire size (i.e. natural gas mass flow rate) increases from top to bottom. *Dashed lines* represent the extent of the door jamb

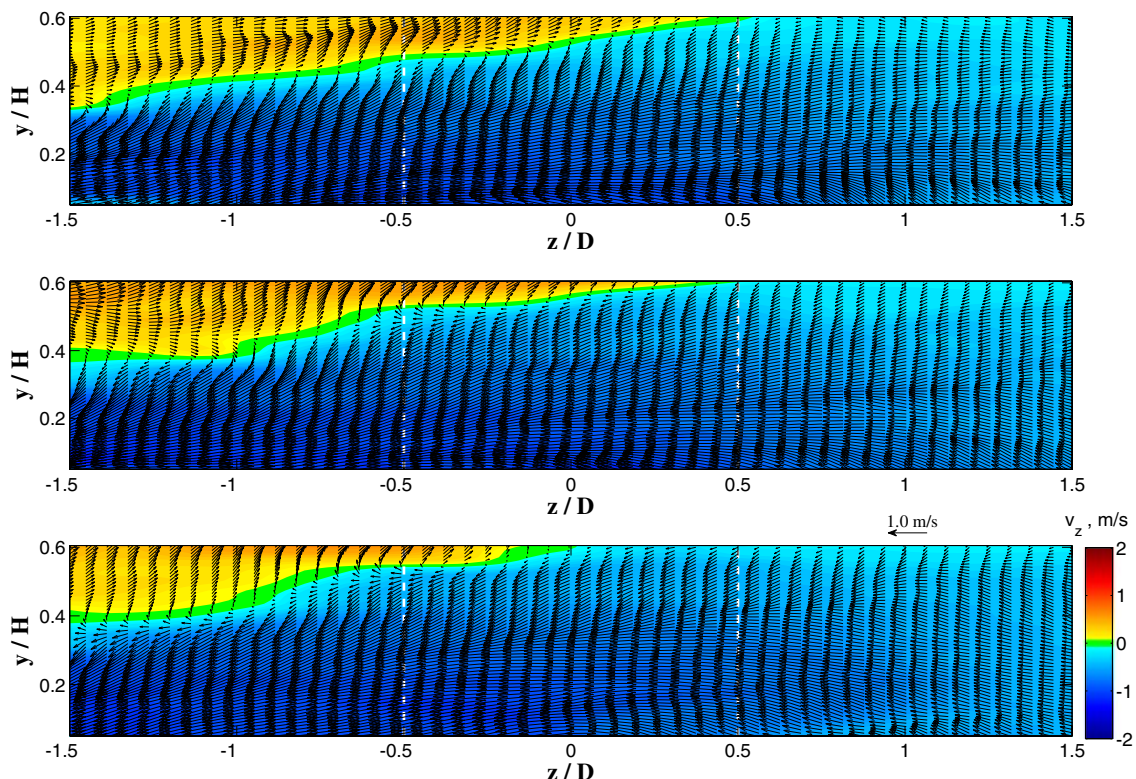


Fig. 11 Instantaneous vector fields along the centerline of the doorway (yz plane, at $x = 0.0$ m), configuration B, 160 kW fire. Starting at the top, the images are sequential and separated in time by 1.0 s

were the greatest in the plane parallel to the laser sheet. This was opposite to configuration A where the primary flow direction and the greatest particle displacements were perpendicular to the laser sheet. In SPIV configuration B a direct measurement of the particle displacement in z was performed; unlike configuration A where the particle displacement in z was inferred from measured displacements in x and y .

The overlap of the measured velocity fields from configurations A and B occurs along a vertical line at $x = 0.00$ m and $z = 0.05$ m. A comparison of the results for v_z along this line is shown in Fig. 12 as the relative difference with respect to measured values from configuration B. The discrepancy between the results is on the order of 3% for the flow below the flow interface and into the room. For the flow above the flow interface and out of the room the discrepancy is greater, on the order of 7%. The larger discrepancy in the region above the flow interface is likely the result of uncertainty in the measurement location in the y coordinate. Due to the larger velocity gradients in y for this region, a small shift in measurement location has a larger impact. The small discrepancy in v_z for the flow below the interface and into the room is within the standard deviation of the repeat measurements. Data in the region of $h \pm 0.1h$ were not included in determining

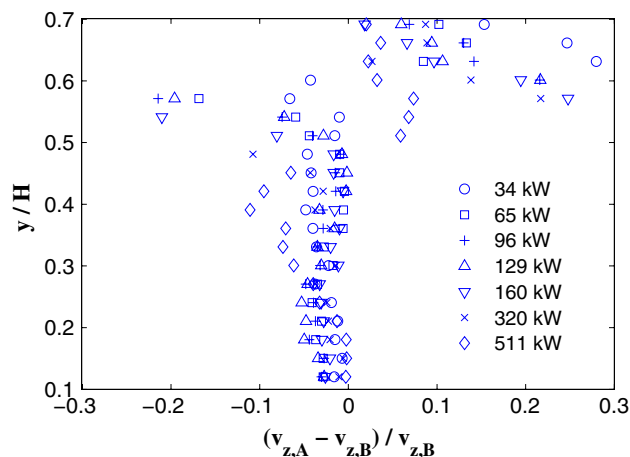


Fig. 12 Comparison of SPIV results for v_z at $x = 0.0$ m and $z = 0.05$ m plotted as the relative difference with respect to configuration B. Fewer data points are displayed for clarity

the average relative differences for the data. This condition was somewhat arbitrary, however, it filtered out the velocity measurements that were close to zero and would amplify the relative difference. These results increase the confidence in large-scale SPIV measurements and demonstrate the level of precision possible in fire experiments.

4 Conclusions

The flow of air through the lower portion of a doorway and available to a fire burning inside a room was fully mapped using SPIV. Measurements were conducted for a series of fires ranging from 34 to 511 kW, which extended the range of fire size when compared to previous detailed studies of doorway flows. This complete mapping of the velocity field allowed an accurate integration to compute the volume flow rate of air into the room. A comparison with computations that apply simplifying assumptions such as flow speed being equivalent to the velocity component normal to the measurement plane and one-dimensional flow demonstrated that the level of error that would result when using such assumptions is less than 5%. The application of these assumptions is analogous to the use of techniques such as a vertical array of bi-directional probes that rely on these simplifying assumptions. These measurements, therefore, provide a benchmark to judge the accuracy of independent measurement techniques with reduced spatial sampling and of more practical usefulness for fire testing. The SPIV measurements provided some previously uncharacterized features of fire-induced flows through a vent. For this experimental configuration the location of zero velocity, the interface of the flow into and out of the enclosure, was a curved region stretching across the width of the doorway for low energy release rate. However, the curvature reduced as the energy release rate of the fire increased. The height above the floor of the interface region is inversely proportional to the energy release of the fire, and it also varies significantly with position through the depth of the doorway. These new observations regarding the location of the flow interface suggest that care should be taken when locating physical probes in the doorway.

The horizontal component of velocity in the direction of the primary flow, v_z , provides the largest contribution to the flow speed at most locations of the flow into the room. However, in regions such as near the flow interface and flow out of the room, the vertical component of velocity was also a significant contributor to the flow speed. Therefore, the assumption that a measurement of flow speed is dominated by flow in the horizontal direction is not always correct. Knowing when and where such conditions exist will be helpful in designing better practical measurement techniques and interpreting existing techniques with limitations on resolving velocity components.

Better than 1% repeatability was demonstrated in achieving the desired experimental conditions from test to test. The standard deviation of the mean of the volume flow rate computed for flow into the room was less than 4% which also reflects very good repeatability in the ability of the SPIV technique to measure the velocity field over such a large spatial domain. A comparison of the results of two

separate configurations using SPIV, each requiring different displacement measurements to compute the same velocity component, demonstrated the ability of SPIV to give precise measurements over a large spatial domain.

Acknowledgments The author wishes to thank Erik Johnsson for data acquisition and Marco Fernandez, Lauren Delauter, Edward Hztensoksy, Jack Lee, and Alexander Maranghides for experimental setup and logistics. The author also wishes to thank the following Summer Undergraduate Research Fellowship Students, Jeff Keslin, Scott Rockwell, and Matthew Smith, for their assistance with data analysis and archiving.

References

- Bryant RA, Mulholland GW (2008) A guide to characterizing heat release rate measurement uncertainty for full-scale fire tests. *Fire Mater* 32:121–139
- Bundy M, Hamins A, Johnsson EL, Kim SC, Ko GH, Lenhert DB (2007) Measurements of heat and combustion products in reduced-scale ventilation-limited compartment fires. NISTTN 1483. National Institute of Standards and Technology, Gaithersburg, Maryland
- Dalziel SB, Lane-Serff GF (1991) The hydraulics of doorway exchange flows. *Build Environ* 26:121–135
- ISO 9705 (1993) Fire tests—full-scale room test for surface products. International Organization for Standardization, Geneva, Switzerland
- Kawagoe K (1958) Fire behavior in rooms. BRI Report 27. Building Research Institute, Ibaraki-Ken, Japan
- Linden PF (1999) The fluid mechanics of natural ventilation. *Annu Rev Fluid Mech* 31:201–238
- McCaffrey BJ, Heskestad G (1976) Robust bidirectional low-velocity probe for flame and fire application. *Combust Flame* 26:125–127
- McCaffrey BJ, Rockett JA (1977) Static pressure measurements of enclosure fires. *J Res Natl Bureau Stand* 82:107–117
- Nakaya I, Tanaka T, Yoshida M, Steckler K (1986) Doorway flow induced by a propane fire. *Fire Saf J* 10:185–195
- Prahl J, Emmons HW (1975) Fire induced flow through an opening. *Combust Flame* 25:369–385
- Prasad AK, Adrian RJ (1993) Stereoscopic particle image velocimetry applied to liquid flows. *Exp Fluids* 15:49–60
- Raffel M, Willert C, Kompenhans J (1998) Particle image velocimetry: a practical guide. Springer, Berlin
- Rockett JA (1976) Fire induced gas-flow in an enclosure. *Combust Sci Technol* 12:165–175
- Steckler K, Quintiere JG, Rinkinen WJ (1982) Flow induced by fire in a compartment. *Proc Combust Inst* 19:913–920
- Steckler K, Quintiere JG, Baum HR (1984) Fire induced flows through room openings: flow coefficients. *Proc Combust Inst* 20:1591–1600
- Sun L, Zhou X, Mahalingam S, Weise DR (2005) Experimental investigation of the velocity field in buoyant diffusion flames using PIV and TPIV algorithm. *Proc Int Assoc Fire Saf Sci* 8:939–950
- Tieszen SR, O'Hern TJ, Schefer RW, Weckman EJ, Blanchat TK (2002) Experimental study of the flow field in and around a one meter diameter methane fire. *Combust Flame* 129:378–391
- Wieneke B (2005) Stereo-PIV using self-calibration on particle images. *Exp Fluids* 39:267–280
- Zhou XC, Gore JP, Baum HR (1996) Measurements and prediction of air entrainment rates of pool fires. *Proc Combust Inst* 26:1453–1459